iomac
International Operational Modal Analysis Conference
11th International Operational Modal Analysis Conference
20 - 23 May 2025 | Rennes, France

Modal shape reconstruction with distributed fiber optic strain sensing

Nicolas Aubert [1], *Vincent Baumann* [2] *and Aghiad Khadour*[1]

[1] Université Gustave Eiffel COSYS-IMSE, Champs sur Marne, France, aghiad.khadour@univ-eiffel.fr
[2] Setec, Paris, France

ABSTRACT
Distributed Fiber Optic Strain Sensing is an family of measurement technologies developed to quantify the local axial strain of an optical fiber. In particular, Optical Frequency-Domain Reflectometry is often used in static structural health monitoring applications thanks to its millimetric spatial resolution and medium range in the tens of meters. This provides a very high number of measurement points while maintaining reasonable cost and complexity. The sensor consists only of a thin fiber optic cable installed inside the studied structure or bonded at its surface. This technique is particularly suitable for measuring the strain distribution of reinforced concrete structures, as the sensing cable can usually be attached at a few points on the bar before pouring the concrete, providing accurate strain transfer and simple sensor installation. In this work we study a planar reinforced concrete structure with a length of 18 meters and a width of 2.6 meters. We placed two straight sensing cables inside the concrete along the length, each one near one side of the structure. The structure is supported on pivots at both ends, and dynamically loaded in flexion. Using the dynamic distributed strain measurements, we characterize the different modes of the structure using a space-frequency representation. This allows us to determine in particular their symmetry. We also demonstrate direct reconstruction of the modes shape and movement of the structure using a simplified shape sensing reconstruction method. We believe this method can be an interesting alternative to discrete conventional sensors when line-of-sight methods cannot be used.

Keywords: modal analysis, fiber optic, shape sensing, distributed sensing

1. INTRODUCTION

The classical approach to measure the eigenmodes of a structure is to use discrete sensors such as accelerometers, strain gauges and linear displacement sensors like LVDTs (Linear Variable Differential Transformer). These systems are cheap, robust and have proven their worth. Their main drawback comes

from their discrete nature. The complexity, reliability and cost of such a system can become problematic when a large number of measurement points are required. Thus it can be attractive to use technologies that inherently provide a greater density of information, with manageable cost and complexity.

Vision-based techniques can be very powerful, as demonstrated in [1]. Their main advantage is that they provide full-field measurements, providing a large number of measurement points with a relatively easy setup and without being intrusive. Sometimes though it is not possible to install a camera-based system, for example because there is not enough space around the structure or because there is no clear view on it. This was the case for this work, as the structure was surrounded by scaffolding that obstructed the lateral viewing angles.

Distributed Fiber Optic Sensing (DFOS) can also provide a great measurement point density with easy setup, but without requiring line-of-sight. DFOS systems work by measuring the local axial strain of an optical fiber. The continuous optical fiber is discretized in a chain of virtual gages of a specific length. In particular, Distributed Acoustic Sensing (DAS) the most evident DFOS technique for dynamic measurements. DAS interrogators can measure dynamic strain down to a $p\varepsilon/\sqrt{Hz}$ with a gage length of a few meters, a bandwidth of several kHz and a range up to 100 km. This makes it possible to easily measure the modes of a structure, even with an optical fiber placed inside a heavily buffered telecom cable inside a service duct. For example, Rodet et al. [2] used a fiber inside a telecom cable that runs inside 5 different bridges over 24 km. The fundamental modes of the bridges could then be measured simply by plugging an interrogator at one end of the fiber. The excitation provided by the environmental noise was sufficient to realize measurements despite the non-ideal mechanical coupling between the fiber and the structures.

If DAS systems are well-suited to monitor large structures thanks to their important range, they can be difficult to use on smaller structures because of the long gage length. In that case, it is possible to use Optical Frequency-Domain Reflectometry (OFDR), which can provide a gage length of less than 1 mm at the cost of a reduced range ($\sim$ 100 m), bandwidth ($\sim$ 100 Hz) and resolution ($\pm 1 \mu\varepsilon$). This lower sensitivity means that the optical fiber used for the measurement must be tightly coupled to the measured structure, like a traditional strain gauge. Another possibility is to use a dedicated fiber optic shape sensor, which only needs to follow the displacement of the structure.This allows direct measurement of the frequencies and shapes of the modes. Lally et al. [3] and Bednarski et al. [4] have demonstrated the use of such shape sensors for metric-scale structures, though only in a static manner.

An important difference between OFDR and DAS is that OFDR measures absolute strain (relatively to a reference measurement), so it is possible to compare measured strain profiles over any period of time. DAS only measures dynamic strain, and integration over long periods can be challenging because of long-term instabilities in the laser source. OFDR is thus well suited for Structural Health Monitoring as it allows direct characterization of the strain of a structure, including cracks or loading evolutions. DAS is better suited to real-time monitoring of events like shocks, and measurement of modal frequencies whose evolution can provide information on the structure's health.

Finally, when high spatial resolution and high acquisition frequency are needed, Fiber Bragg Gratings (FBG) can be an interesting solution [5], as they can be made down to a few millimeters in length and measured up to the MHz range. The main downside is that, compared to DAS and OFDR we lose the ability to use standard optical fibers. With an FBG system, we need to either install and connect discrete FBGs, or use a custom-made optical fiber with FBGs inscribed in it which can be quite expensive.

In this work, we chose to use OFDR because it works with standard optical fibers and has a spatial resolution and sensing range that are adapted to the studied structure.

2. EXPERIMENTAL SETUP

The studied structure is 18 meters long by 2.6 meters wide, made of a thin reinforced concrete slab and supported by two steel beams as shown in Figure 1. Some additional smaller concrete slabs are

bolted onto the structure to act as weights. The structure is supported on pivot points at its extremities to allow for flexion. Optical fibers are embedded in the concrete slab, in the form of two straight segments of a specific fiber optic sensing cable, on each side of the structure throughout its entire length. The fibers are placed above the neutral fiber, so the strain of the fibers will have the same sign as the vertical displacement of the structure.

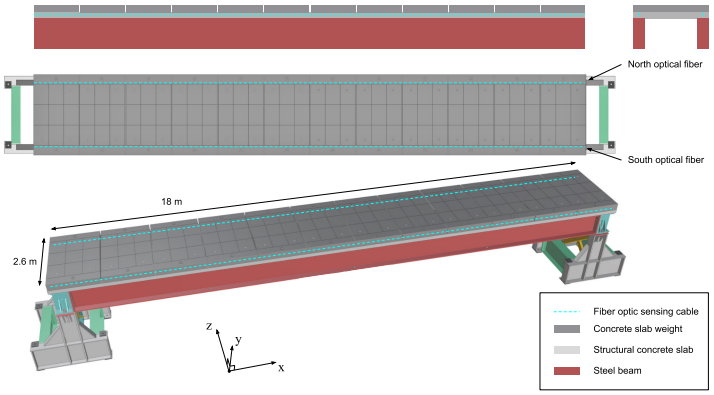

Figure 1: Views of the studied structure and the placement of the sensing cables. Courtesy of Setec.

The two straight optical fibers are approximately 20 m long. The length of the structure is only 18 m but we needed approximately 1 m on each side as margin for connectorization and termination of the optical fibers. The interrogator we used (Luna ODiSI 6104) can run at 50 Hz with up to 20 m of optical fiber on one channel, so that two 20 m fibers can be measured sequentially at 25 Hz.

Another possibility would have been to join the two fibers and to use only one channel, but in this case the maximum frequency of the interrogator would have been only 20 Hz, and we would have lost some reliability and flexibility (possibility of measuring only one fiber at 50 Hz for example), so we went with two channels. We considered a Nyquist frequency f_{Ny} of 12.5 Hz to be sufficient for this work, since the 3 first modes of the structure are expected to be around 4.6, 7.3 and 9.7 Hz (frequencies obtained through FEM simulation). These modes are respectfully flexion, torsion and torsion. The second mode of flexion is estimated at 14.5 Hz so we shouldn't be able to measure it with the two channels at 25 Hz. However, as we will show in the results we were actually able to measure it thanks to aliasing.

The structure was excited by vertical-moving mass actuators evenly distributed over the whole surface of the structure, i.e. people jumping at the rhythm of a metronome. The reasons for this go beyond the scope of this work and are detailed in the PhD thesis of Vincent Baumann [6]. In this work we will focus only on the information we can recover on the structure's behavior from the fiber optic strain data.

3. FREQUENCY ANALYSIS

The first step to study the modes is to measure their frequency, by looking for peaks in the strain data spectra. To get these frequencies we applied Fast Fourier Transform to the strain measurements of a few gages near the middle of the structure. As shown in Figure 2, the spectrum of a single gage is too noisy to see mode 3 around 9.7 Hz, because its magnitude is much lower than the noise floor. So to lower the noise floor we apply the FFT to the average strain of a group of gages around the middle point, where the displacement of the structure is the highest and so where the magnitude of the strain will be the highest. This is important because the magnitude of the measured strain is at most only around 10 times the amplitude of the noise level, so it is important to select the most favorable placement. We ultimately chose a window of 401 points, as this gave us the lowest noise floor we could obtain while still keeping a reasonable spatial resolution at around one meter. To make the plots more readable we also smooth the spectral data with a 5σ Gaussian filter.

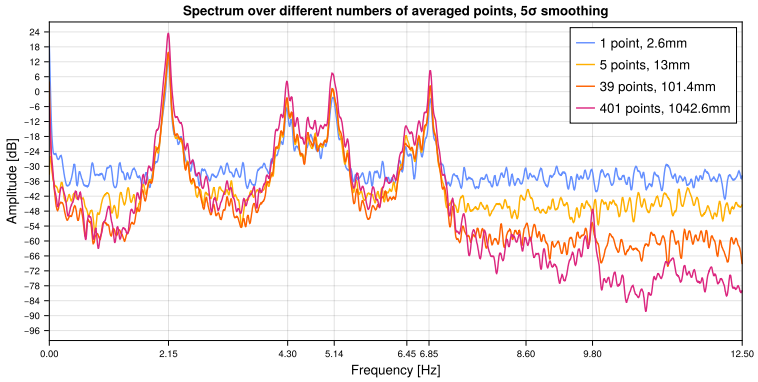

Figure 2: Comparison between spectra of one and several averaged points

Looking at Figure 2 we clearly see 4 main peaks at 2.15, 4.30, 5.14 and 6.85 Hz. A smaller fifth one is visible at 9.80 Hz thanks to the spatial downsampling. We know that the 2.15 Hz peak corresponds to the frequency of excitation because it was the tempo of the metronome (129 beats per minute). The one at 4.30 Hz is obviously the second harmonic of the excitation. So we can deduce that 5.14 Hz is the frequency of Mode 1, as it cannot be an excitation harmonic and it is relatively close to the simulation result. The third harmonic of the excitation is at 6.45 Hz and visible close to the 6.85 Hz peak. Hence the 6.85 Hz peak should correspond to Mode 2. The fourth excitation harmonic at 8.60 Hz is not clearly visible here, and finally the small peak at 9.80 Hz should be Mode 3. Mode 4 is a special case, because according to the simulation it should be beyond the Nyquist frequency of the measurement which is 12.5 Hz, since the strain data was acquired at 25 Hz. So according to the simulation it would be folded at around 10.5 Hz, where nothing appears clearly on the plot. However that is expected since this mode presents a null at the middle of the structure. This behavior is further explored with the space-frequency representation. We see that it is clearly possible to extract useful data from a simple spectrum, using the help of insider information about the excitation and the structure. However we can go further in the analysis by using the two fibers we have installed instead of only one.

3.1. Differential Spectra

The two optical fibers are installed near the edges of the structure along its length, symmetrically from its middle axis. So for a symmetric mode like a flexion mode (Mode 1 and 4) the strain of both fibers should be in phase. As such, the frequency peak of the mode should disappear in the spectrum of the differential strain of the two fibers. By differential strain we mean that we compute the spectrum of the difference between the strains of the two fibers. Conversely, the strains of an anti-symmetric mode (like a torsion mode, see Mode 2 and 3) should be perfectly out-of-phase. And so its peak should disappear in the spectrum of the average strain of the two fibers. This should make it easy to identify the type of mode for each peak. Additionally, we know that the excitation is a bit chaotic since the people jumping on the structure are not perfectly in sync. If it were the case, with an evenly distributed periodic load the excitation bands would be perfectly symmetric, and so they would disappear in the differential spectrum. But here, over the duration of the test (4 minutes) the excitation strains of the two fibers have no reason to be perfectly in phase so the excitation bands should be still visible in the differential spectra.

After precise synchronization of the measurements of both fibers we can clearly see on Figure 3 the differential 5.14 Hz band disappearing, and the same for the average 6.85 and 9.80 Hz bands, indicating that these modes are indeed respectfully flexion, torsion and torsion. Now, rigorously this only tells us if the modes are symmetric or anti-symmetric, and an in-plane flexion mode would also be anti-symmetric. But with this particular structure, because of its relatively low aspect ratio and because of the direction of excitation we do not expect to have measurable in-plane flexion modes, so we can consider

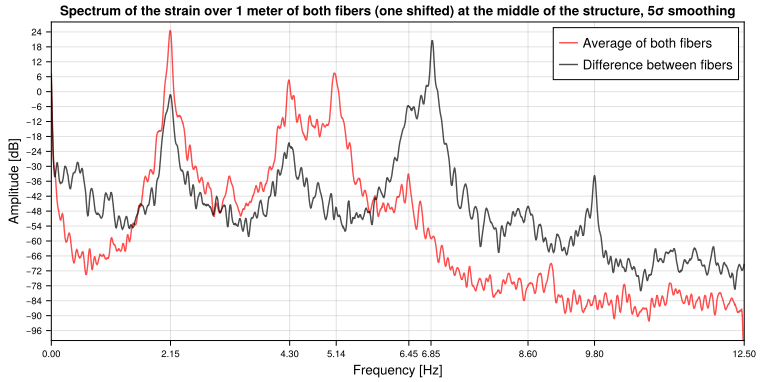

Figure 3: Comparison of the spectra of symmetric and anti-symmetric modes

anti-symmetric modes to be torsion modes.

This approach is useful to have an idea of the shape of the modes, although that is only possible with the modes visible at the one position of interest.

3.2. Space-Frequency Representation

The 2D space-frequency representation makes better use of the distributed nature of fiber sensing by showing the spectra at each measurement point along the structure. Because of the noise level we do the same as above : for each point we take the median of the strain inside a window of 401 points centered on the considered gage. We then compute the spectrum of these averaged strains, and repeat the operation over the whole useful length of the optical fiber. Figure 4 presents the result of this space-frequency representation for one fiber. As expected the main peaks visible in Figure 2 appear as strong and continuous horizontal lines.

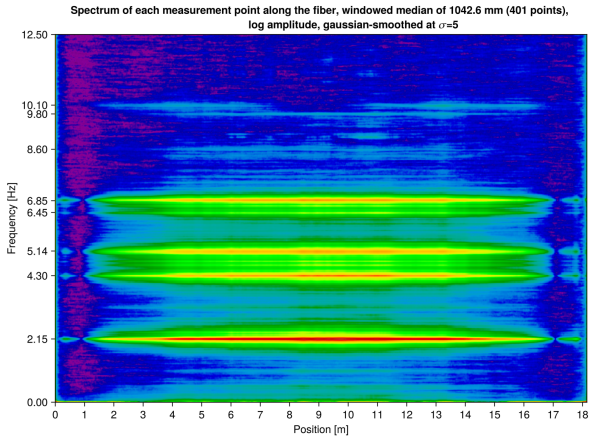

Figure 4: S-f plot of the strain of one fiber at 25 Hz

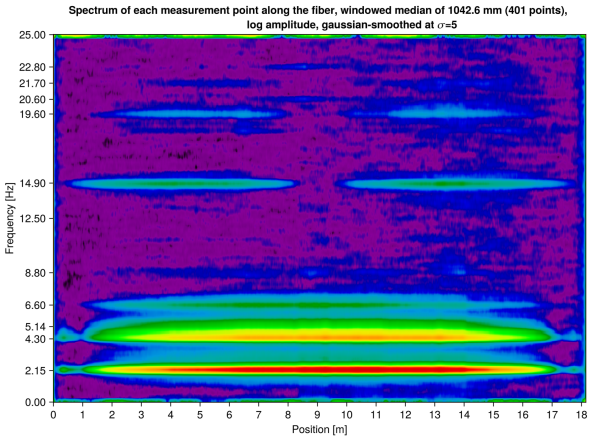

Figure 5: S-f plot of the strain of one fiber at 50 Hz

This is because they are all first order modes, meaning they have only one antinode. However the line at 10.10 Hz is different, it vanishes near the middle of the structure as if it was made of two distinct parts — or two antinodes. This what we would expect from a second order mode like Mode 4, but it has been simulated at 14.46 Hz and until here the simulation has been quite accurate. However, 10.10 Hz is the frequency at which a 14.90 Hz line would appear if sampled at 25 Hz like here, because of frequency aliasing. Frequency aliasing is rarely a problem with traditional acoustic or electric measurements because these systems often include anti-aliasing filters. However this is not the case with the system used

in this work.

Figure 5 confirms that is it indeed a 14.90 Hz line that is folded at 10.10 Hz. This is the same representation as before but for a measurement that was done at 50 Hz. This is possible with only one fiber measured at a time, so we did only one test at 50 Hz. But it is enough to confirm the frequency of Mode 4. More modes are visible beyond 15 Hz, but they seem mostly covered by the other modes in the 25 Hz measurement. We were quite lucky that aliased Mode 4 did not ended up superposed with another mode, otherwise we wouldn't have been able to isolate it. This shows the importance of keeping frequency aliasing in mind while analyzing frequency data. It is often a source of problems, but with a bit of luck it can also by an opportunity to measure phenomena that exceed our expected measurement ability.

This allowed us to confirm the frequency of Mode 4, however its symmetry is uncertain for now since it is not apparent in the differential spectra we previously calculated in Figure 3. We can then simply plot the Space-Frequency representation of average and differential strain (respectively Figures 6 and 7).

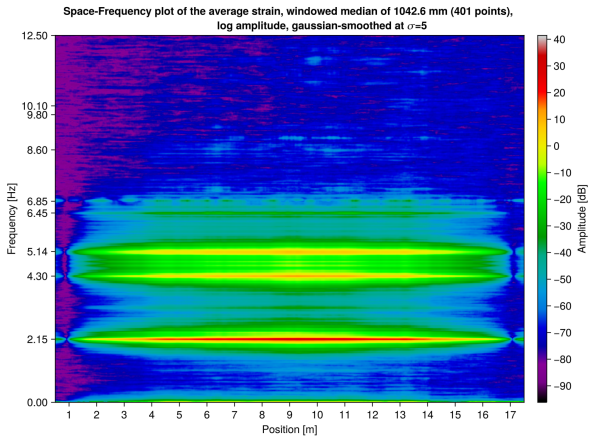

Figure 6: S-f plot of the average strain

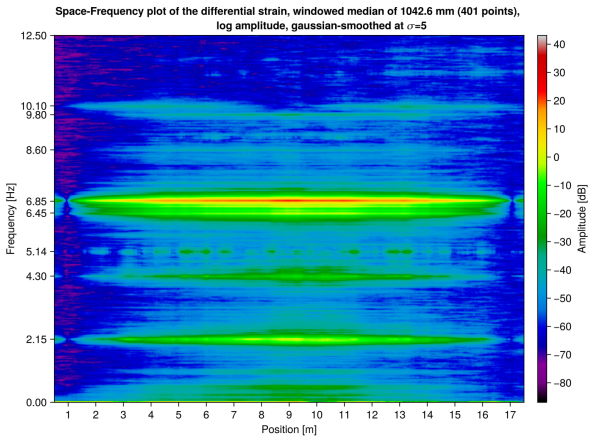

Figure 7: S-f plot of the differential strain

We see that the 10.10 Hz line doesn't appear on the average strain plot, but it is present in the differential strain data. This indicates that this mode is in fact an anti-symmetric mode as opposed to the result of the simulation. The second-order flexion mode might be at 19.60 Hz visible in 5, but we cannot confirm as we could only measure one fiber at a time at this frequency. As for the other three modes (5.14, 6.85 and 9.80 Hz) the conclusions are unchanged.

4. SHAPE RECONSTRUCTION

4.1. Shape Reconstruction Algorithm

The general concept of fiber optic shape sensing is to equip a structure with fiber optic strain sensors such that we can obtain local axial strain data at several locations in each section of the structure. We can then apply simple trigonometry to obtain the local bending direction and magnitude, following the principles of beam theory. The global three-dimensional shape of the structure is then computed by integrating all the discrete curvatures over its length, with respect to a chosen origin direction. In this work we use a simplified algorithm similar to the one used by Bednarski et al. [4].

The first steps of the general-case algorithm are illustrated in 8. At least 3 measurements points are needed at each section of the measured path. The sensing points are placed in their respective positions in the zy plane, and displaced along the x axis according to their measured strain. The normal vector of the plane intersecting the 3 points is then scaled by the sensing length used for the strain measurement, and added to the reconstructed shape. This procedure is applied for every section of the measured shape from one end to the other.

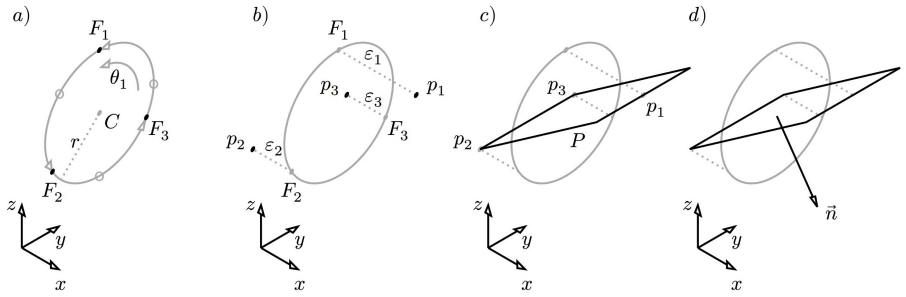

Figure 8: Comparison of the spectra of symmetric and anti-symmetric modes

In our case, we consider each one of our two optical fibers to be only deformed along their vertical plane, because of the shape of the structure and the type of excitation. Therefore, using the configuration shown in 8, we assign the strain measured by the fiber ε to ε_1, and $-\varepsilon/2$ to ε_2 and ε_3, to emulate a structure subjected to pure vertical deflection. The shape of both fibers is independently reconstructed, and then simple interpolation is used to fill the space between them to represent the deformed shape of the structure, as presented in 9. For these plots, the strain data is filtered by a narrow band-pass filter to isolate the strain caused by each mode. The shape reconstruction then allows for proper identification of the modal shapes. The results are coherent with the space-frequency representation because of the simplicity of the structure's shape, but would be especially helpful in the case of a complex structure using a dedicated shape-sensing system.

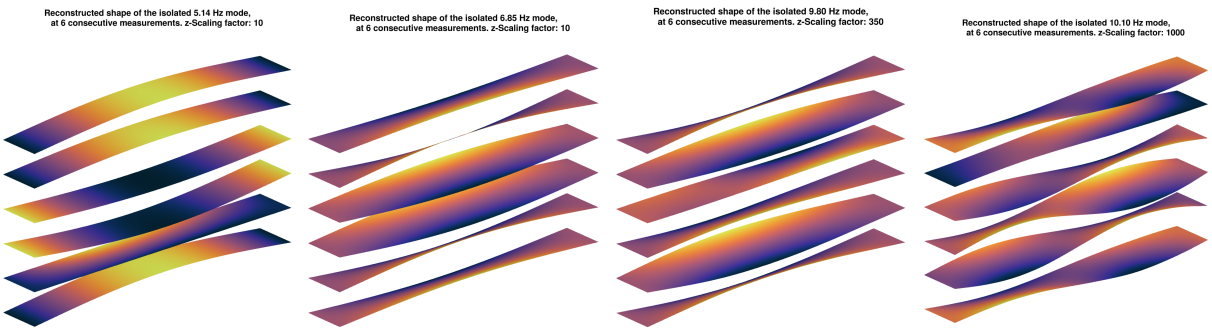

(a) 5.14 Hz, x10 **(b)** 6.85 Hz, x10 **(c)** 9.80 Hz, x350 **(d)** 14.90 Hz, x1000

Figure 9: Reconstructed shape of the first 4 modes at 6 successive acquisitions with their respective z-scaling factor.

5. CONCLUSIONS

In this work we demonstrated an innovative use of OFDR for dynamic strain measurements, and how it can be used in conjunction with shape sensing to study the shape changes and eigenmodes of a structure at high spatial resolution without requiring line of sight sensors. Taking into account the intrinsic advantages of fiber optic sensing this could be a useful tool for modal analysis and structural monitoring for applications with specific requirements.

ACKNOWLEDGMENTS

The authors are grateful to M. Vincent Baumann and the company Setec for the opportunity to work on this experiment, which was realized as part of M. Baumann's PhD thesis on crowd-structure interactions.

REFERENCES

[1] Javad Baqersad, Peyman Poozesh, Christopher Niezrecki, and Peter Avitabile. Photogrammetry and optical methods in structural dynamics – a review. *Mechanical Systems and Signal Processing*, 86: 17–34, 2017. ISSN 0888-3270. doi: https://doi.org/10.1016/j.ymssp.2016.02.011. URL https://www.sciencedirect.com/science/article/pii/S0888327016000388. Full-field, non-contact vibration measurement methods: comparisons and applications.

[2] Julie Rodet, Benoit Tauzin, Mohammad Amin Panah, Philippe Guéguen, Destin Nziengui Bâ, Olivier Coutant, and Stéphane Brûlé. Urban dark fiber distributed acoustic sensing for bridge monitoring. *Structural Health Monitoring*, 2024. doi: 10.1177/14759217241231995.

[3] Evan M. Lally, Matt Reaves, Emily Horrell, Sandra Klute, and Mark E. Froggatt. Fiber optic shape sensing for monitoring of flexible structures. In Masayoshi Tomizuka, Chung-Bang Yun, and Jerome P. Lynch, editors, *Sensors and Smart Structures Technologies for Civil, Mechanical, and Aerospace Systems 2012*, volume 8345, page 83452Y. International Society for Optics and Photonics, SPIE, 2012. doi: 10.1117/12.917490. URL https://doi.org/10.1117/12.917490.

[4] Łukasz Bednarski, Rafał Sieńko, Marcin Grygierek, and Tomasz Howiacki. New distributed fiber optic 3dsensor with thermal self-compensation system: Design, research and field proof application inside geotechnical structure. *Sensors*, 21(15):5089, January 2021. ISSN 1424-8220. doi: 10.3390/s21155089. URL https://www.mdpi.com/1424-8220/21/15/5089.

[5] Jeannot Frieden, Joël Cugnoni, John Botsis, Thomas Gmür, and Dragan Ćorić. High-speed internal strain measurements in composite structures under dynamic load using embedded fbg sensors. *Composite Structures*, 92(8):1905–1912, 2010. ISSN 0263-8223. doi: https://doi.org/10.1016/j.compstruct.2010.01.007. URL https://www.sciencedirect.com/science/article/pii/S0263822310000103.

[6] Vincent Baumann. Crowd-structure interaction on building floors for event use, October 2024. URL https://hal.science/hal-04906126.